



NEXT GENERATION PEM ELECTROLYSERS UNDER NEW EXTREMES

HORIZON 2020 PROGRAMME
FUEL CELLS AND HYDROGEN JOINT UNDERTAKING (FCH 2 JU)

Grant agreement no.: 779540

Start date: 01.02.2018 – Duration: 36 months

Project Coordinator: Rachel Backhouse – ITM

DELIVERABLE REPORT

D5.3 – PUBLIC REPORT ON MEA DEVELOPMENT AND CHARACTERISATION		
Due Date	30-April-2020	
Authors	S. Siracusano, N. Briguglio, F. Pantò, M. Bottari, A.S. Aricò (CNR-ITAE) L. Grahl-Madsen (IRD)	
Work package	WP5	
Work package Leader	5 - IRD	
Lead Beneficiary	5 - IRD	
Date released by WP leader	21 April 2020	
Date released by coordinator	28 April 2020	
DISSEMINATION LEVEL		
PU	Public	X
PP	Restricted to other programme participants (including the Commission Services)	
RE	Restricted to a group specified by the consortium (including the Commission Services)	
CO	Confidential, only for members of the consortium (including the Commission Services)	
NATURE OF THE DELIVERABLE		
R	Report	X
D	Demonstrator	
O	Other	

SUMMARY			
Keywords	Electrolysis, Polymer electrolyte membranes, Electro-Catalysts, MEAs, Stack, Characterisation, Procedures, Protocols		
Abstract	<p>The activities reported in this deliverable regard MEA development studies carried out in the FCH JU Neptune project. Specific efforts were addressed to optimising catalyst ink composition and improving the procedure of ultrasonic catalyst coating on membranes for ultra-low catalyst loadings (IRD). The catalyst ink optimisation activity was addressed to tailor catalyst-ionomer composites as a function of ionomer equivalent weight and catalyst morphology to extend the reaction interface and favour a high degree of catalyst utilisation (CNR). These were pre-requisite to achieve MEA performance of 4 A cm^{-2} at 1.75 V using an ultra-low PGM loading $< 0.4 \text{ mg cm}^{-2}$ MEA (project target). The improvements were also addressed to minimise waste and improve stability. An iterative approach included optimisation of amount of solvent, additives and processing parameters used.</p> <p>MEA characterisation was used to screen the different formulations and preparation procedures and served to assess the achievement of the project targets (CNR). Electrochemical and physico-chemical characterisation addressed to provide insights into the optimal electrode structure (CNR). The aim was to maximize electrochemically active surface area, minimize losses due to transport of charge carriers as well as reactants and products. Electrochemical testing included:</p> <ul style="list-style-type: none"> - Single cell testing in a wide range of temperatures (from ambient to $140 \text{ }^{\circ}\text{C}$) and pressures (from ambient to 20 bar) as well as in a wide range of current densities (up to 8 A cm^{-2}) - Determination of gas permeation using high sensitivity gas sensors and gas chromatographic analysis to evaluate the capability of the recombination catalysts inside the MEAs to manage gas permeation at high pressure. 		
Public abstract for confidential deliverables	Public		
REVISIONS			
Version	Date	Changed by	Comments
0.1	01-04-2020	Stefania Siracusano (CNR)	First draft
0.2	02-04-2020	Antonino Aricò (CNR)	Implementation
0.3	28-04-2020	Rachel Backhouse (ITM)	Final draft

Disclaimer/ Acknowledgment



Copyright ©, all rights reserved. This document or any part thereof may not be made public or disclosed, copied or otherwise reproduced or used in any form or by any means, without prior permission in writing from the NEPTUNE Consortium. Neither the NEPTUNE Consortium nor any of its members, their officers, employees or agents shall be liable or responsible, in negligence or otherwise, for any loss, damage or expense whatever sustained by any person as a result of the use, in any manner or form, of any knowledge, information or data contained in this document, or due to any inaccuracy, omission or error therein contained.

All Intellectual Property Rights, know-how and information provided by and/or arising from this document, such as designs, documentation, as well as preparatory material in that regard, is and shall remain the exclusive property of the NEPTUNE Consortium and any of its members or its licensors. Nothing contained in this document shall give, or shall be construed as giving, any right, title, ownership, interest, license or any other right in or to any IP, know-how and information.

This project has received funding from the FCH JU and European Union's Horizon 2020 research and innovation programme under grant agreement No 700008. This Joint Undertaking receives support from the European Union's Horizon 2020 research and innovation programme and Hydrogen Europe, and Hydrogen Europe Research

The information and views set out in this publication does not necessarily reflect the official opinion of the European Commission. Neither the European Union institutions and bodies nor any person acting on their behalf, may be held responsible for the use, which may be made of the information contained therein.

CONTENTS

1. INTRODUCTION.....	6
2. EXPERIMENTAL	7
2.1 Materials	7
2.2 Physico-chemical characterisations	8
2.3 Preparation of catalyst-coated membrane	8
2.4 Electrochemical measurements	9
3. RESULTS AND DISCUSSION	10
3.1 Microstructure and morphology of the unsupported PtCo recombination catalyst	10
3.2 Surface characterisation of the PtCo catalyst	11
3.3 Single cell electrochemical assessment of the Pt-Co alloy catalyst for the reduction of the hydrogen concentration in the oxygen stream	12
4. CONCLUSIONS.....	23
Acknowledgements	23

LIST OF ACRONYMS, ABBREVIATIONS AND DEFINITIONS

Abbreviation	Explanation
ADF	<u>A</u> msterdam <u>D</u> ensity <u>F</u> unctional
BET	<u>B</u> runauer– <u>E</u> mmett– <u>T</u> eller
BF	<u>B</u> right <u>F</u> ield
CCM	<u>C</u> atalyst <u>C</u> oated <u>M</u> embrane
CL	<u>C</u> atalyst <u>L</u> ayer
CNT	<u>C</u> arbon <u>N</u> ano <u>T</u> ubes
DMF	<u>D</u> i <u>M</u> ethyl <u>F</u> ormamide
ECSA	<u>E</u> lectro <u>C</u> hemical <u>S</u> urface <u>A</u> rea
EDX	<u>E</u> nergy-dispersive X-ray spectroscopy
EIS	<u>E</u> lectrochemical <u>I</u> mpedance <u>S</u> pectroscopy
EW	<u>E</u> quivalent <u>W</u> eight
FC	<u>F</u> uel <u>C</u> ell
FRA	<u>F</u> requency <u>R</u> esponse <u>A</u> nalysers
GDL	<u>G</u> as <u>D</u> iffusion <u>L</u> ayer
MEA	<u>M</u> embrane <u>E</u> lectrode <u>A</u> ssembly
PAN	<u>P</u> oly <u>A</u> crylo <u>N</u> itrile
PEM	<u>P</u> roton <u>E</u> xchange <u>M</u> embrane
PFSA	<u>P</u> er <u>F</u> luoro <u>S</u> ulfonic <u>A</u> cid
SEM	<u>S</u> canning <u>E</u> lectron <u>M</u> icroscope
STEM	<u>S</u> canning <u>T</u> ransmission <u>E</u> lectron <u>M</u> icroscope
TEM	<u>T</u> ransmission <u>E</u> lectron <u>M</u> icroscopy
TGA	<u>T</u> hermo <u>G</u> ravimetric <u>A</u> nalysers
XPS	<u>X</u> -ray photoelectron spectroscopy
XRD	<u>X</u> -ray diffraction

1. INTRODUCTION

Hydrogen produced by electrolysis has recently gained significant attention as an energy carrier to store the excess of electricity produced by renewable energy sources that cannot be fed into the grid. The storage of hydrogen at high volumetric energy density, e.g. as liquid (cryogenic) hydrogen, requires large energy consumption and technical safety assessment. Instead, the approach of a direct production of pressurized hydrogen from electrolytic water splitting appears very attractive. This can allow saving relevant amounts of energy being the electrochemical compression, according to the Nernst law, much more efficient than the mechanical gas compression. The latter is consuming about 20% of the overall energy involved in the transformation cycle from liquid water to hydrogen gas pressurised at about 700 bar as needed for refuelling modern fuel cell vehicles. Polymer electrolyte membrane (PEM) electrolyzers are in principle able to produce hydrogen at very high pressure thus reducing the post-compression energy consumption. These systems are also relatively compact since they operate at high current density and are characterised by proper dynamic behaviour for grid-balancing service and direct interface with renewable power sources.

One of the main factors limiting the efficiency of PEM electrolyzers is that at high current density e.g. 3 A cm^{-2} (corresponding to high production rates), ohmic losses dominate the overall behaviour with about 85% of polarisation losses. These losses are mainly associated to the use of thick perfluoro sulfonic acid (PFSA) membranes, like Nafion® 117 membrane. Thick membranes are used to provide a barrier to H_2 crossover under high-pressure operation avoiding formation of explosive mixtures at the anode compartment.

On the other hand, a thin membrane can reduce the ohmic resistance of an electrolysis system allowing to increase the current density at a specific voltage efficiency. This allows a decrease of capital costs which are inversely related to the hydrogen production rate.

However, the voltage efficiency (ratio between thermoneutral potential and cell voltage) decreases by increasing the current density as more heat is released into the atmosphere by the electrolysis system. Alternatively, at nominal operating current density, a thin membrane would result in a decrease of ohmic losses thus increasing the voltage efficiency. The cost of green electrolytic hydrogen production is affected by both the capital costs of the electrolysis system (CAPEX) and operating costs (OPEX). The OPEX impact is mainly related to the renewable electricity cost. Thus, an increase of the process efficiency is highly desirable.

Gas permeability in the PFSA membranes is largely related to membrane thickness, permeability and operating temperature. Thin membranes cause a large increase of gas crossover especially when the cell operates under asymmetric (differential) pressure conditions and at high temperature.

In several commercial PEM electrolyzers, the cathode compartment is pressurized whereas the anode stream is kept at ambient pressure. This avoids the oxidation of the current collectors made in titanium and increases the safety conditions (fire and explosion hazards are amplified by the presence of pressurised oxygen). An asymmetric working pressure of 30-40 bar is considered a trade-off between the need to pressurise hydrogen and the technological requirements (e.g. in terms of design and sealing).

The effects of hydrogen permeation towards the anode are mostly evident at low partial loads (below 20%). When the current density is low, the dilution effect by the produced oxygen is also small and the hydrogen concentration in the oxygen stream is high. For safety reasons, an electrolysis system is shutdown when the hydrogen concentration in oxygen reaches 2-3 %. Commercial PEM electrolyzers usually consist of a thick (170 μm) Nafion 117 membrane separator to offer a physical barrier to hydrogen permeation at high pressure. A reduction of the membrane thickness can provide a simple and effective option to increase the current density and reduce the capital costs. However, this approach requires, in parallel, a mitigation strategy to minimize the hydrogen concentration in the oxygen stream, especially at low partial loads.

In the literature, several reports have addressed a better comprehension of hydrogen crossover and related issues. With regard to oxygen permeation to the cathode, an external catalytic gas recombiner (deoxygenation catalytic recombiner or deoxo) converts the traces of permeated oxygen into water through a H_2/O_2 recombination process. To mitigate the hydrogen crossover, the strategies developed until now have been based on the modification of membrane structure by the use of Pt nanoparticles, specific fillers or nanofibrous reinforcements. The use of a Pt electrode layer in between two membranes has also been reported in literature.

The present study instead explores the concept of a recombination catalyst similar to that used in a deoxo system but integrated in a membrane-electrode assembly (MEA). In particular, the recombiner is used inside the anode where permeated hydrogen meets evolved oxygen. To avoid flammability occurrence in PEM electrolyzers, the

recombiner characteristics and operating conditions are essentially different from those of a conventional Pd/Al₂O₃ catalyst used in a deoxo system for purification purposes. The latter operates in the context of a chemical process occurring inside a packed bed reactor that is fed with a hydrogen stream containing traces of oxygen. Whereas, for the recombination catalyst integrated in the MEA, beside a good activity, other requisites are needed. These regard a proper electronic conductivity, a good capability to sustain oxidising conditions (a reducing environment is instead occurring for the hydrogen stream passing through the deoxo) and the need to avoid interfering with the oxygen evolution.

In this study, we show the progress achieved in comparison to our previous activity (D4.3) where a Pt-alloy catalyst was integrated in the anode of an electrolysis MEA and investigated as hydrogen oxidation catalyst. The present advances deal with both catalyst properties and MEA configuration. Moreover, PEM electrolyser operation at intermediate temperatures (140°C) under pressurised conditions was explored because of the enhanced reactions kinetics and lower cooling requirements.

In the previous activity (D4.3), a Pt-Co alloy was deposited over an Aquivion® perfluoro sulfonic acid membrane (90 µm) forming thus an interlayer between the membrane and a conventional IrRuOx anode catalyst layer deposited on the outer surface of the Pt-alloy. Ir-oxide based catalysts are widely used for the oxygen evolution in PEM electrolysis. Our previous activity showed promising activity of the PtCo catalyst in reducing the hydrogen content in an oxygen stream especially when this was investigated out-of-cell in a gas-phase packed-bed catalytic reactor (99.5%). However, a lower performance was recorded when the oxidation catalyst was integrated in the membrane-electrode assembly. This was attributed to the prevalence of an electrochemical oxidation mechanism for the permeated hydrogen compared to the pure recombination mechanism of H₂ and O₂ into water that occurred in the catalytic packed bed reactor. Based on the previous results, the aim of the present study was to improve the catalyst properties in relation to the recombination process and its integration in the MEA. In particular, to exploit better the PtCo catalyst's functionality, this was mixed with a conventional IrRuOx catalyst and deposited over the membrane to form a composite anode layer (MEA: cathode/membrane/mixed IrRuOx-PtCo anode). This configuration was compared with the previous configuration where the PtCo alloy was located in between the membrane and the IrRuOx oxygen evolving layer forming a double layer anode (MEA: cathode/membrane/ PtCo hydrogen oxidation layer/ IrRuOx oxygen evolving layer).

The nanosized PtCo catalyst used for both the composite (mixed) and double layer (unmixed) anode was an improved version of our previous unsupported PtCo alloy. In particular, a different preparation procedure was used to obtain a catalyst with larger degree of alloying between Pt and Co and a smaller crystallite size.

Moreover, the properties of PtCo for reducing the hydrogen concentration in the anodic steam were assessed in the presence of a thinner PFSA membrane (50 µm) characterised by larger gas permeation rate compared to the membranes used in our previous activity (90 µm) (D4.3). This allowed to assess the catalytic system under more harsh operating conditions as well as to explore the possibility of using thin polymer electrolyte membranes in PEM electrolysis as a useful approach to reduce ohmic losses and enhance the voltage efficiency.

2. EXPERIMENTAL

2.1 MATERIALS

The new recombination catalyst here synthesized was a nanosized unsupported Pt-Co alloy (85:15 at. %). The synthesis of the catalyst was carried out according to the sulphite complex route (D4.1). Platinum and cobalt sulphite precursors, in the selected stoichiometric amounts, were neutralised with sodium hydroxide and then oxidised with hydrogen peroxide. The solution was stirred overnight and the pH was adjusted with sodium hydroxide. Colloid formation and successive solid precipitation occurred upon heating the solution at 70° C. The obtained amorphous oxides mixture was then washed, filtered and dried in air at room temperature. The post-synthesis treatments consisted of a reduction step, in order to promote the alloy formation, and a pre-leaching process, in order to remove both impurities and unalloyed Co atoms from the surface of the catalyst. With respect to our previous Pt-Co alloys (D4.3), in this work, a lower reduction temperature and an acidic pre-leaching treatment, in a solution five times more concentrated than the previous one were used. These conditions were selected after an optimisation procedure, in order to obtain a Pt-Co catalyst with smaller crystallite size and lower content of unalloyed Co species. The catalyst was reduced in diluted hydrogen (10% vol. H₂ in helium at 150 °C).

Thereafter, it was pre-leached in 0.5 M perchloric acid at 80° C. The catalyst was finally milled at 300 rpm to improve its morphology for the spray deposition process during the MEA manufacturing.

2.2 PHYSICO-CHEMICAL CHARACTERISATIONS

The structural analysis was performed by using a Philips X-Pert diffractometer equipped with a CuK α as radiation source. The diffraction patterns were interpreted by means of the Joint Committee on Powder Diffraction Standards (JCPDS).

The morphology was investigated by scanning electron microscopy (SEM) and transmission electron microscopy (TEM). SEM was carried out by a FEI S-FEG XL30 microscope equipped with energy dispersive X-ray (EDX) spectrometer, in order to quantify the bulk elemental composition. Transmission electron microscopy (TEM) was performed with a FEI CM12 microscope; catalysts were dispersed in isopropyl alcohol and deposited on a carbon-coated copper grid.

The surface composition was obtained through an X-ray photoelectron spectroscopy analysis by using a PHI 5800-01 spectrometer. Spectra were collected using a monochromatic Al K α X-ray source and acquired with a pass energy of 187.85 eV for survey and 11.75 eV for high resolution spectra, respectively.

2.3 PREPARATION OF CATALYST-COATED MEMBRANE

Membrane-electrode assemblies were prepared by using the catalyst-coated membrane (CCM) approach. The specific properties of the electrocatalysts are reported in Table 1 along with the corresponding bulk and surface composition, the crystallographic structure and crystallite size.

Catalyst	Bulk composition	Surface composition	Crystallographic Structure	Crystallite Size (nm)
Anode	Ir _{0.7} Ru _{0.3} O _x	Ir _{0.8} Ru _{0.2} O _x	Tetragonal	7.9
Cathode	40 % Pt/C	40 % Pt/C	Pt cubic and Carbon support hexagonal	3.3
Recombination Catalyst	Pt _{0.85} Co _{0.15}	Pt _{0.9} Co _{0.1}	Cubic	4

Table 1. Anode, cathode and recombination catalyst and their physico-chemical properties.

A commercially available melt-extruded membrane, Solvay Aquivion® membrane (E98-05S) with an equivalent weight (EW) of 980 g eq⁻¹ and a thickness of 50 μ m was used as membrane separator. A 40% Pt/C (Ketjenblack® carbon) was used for hydrogen evolution whereas IrRuOx (70:30 at.) was used as anode catalyst for oxygen evolution. The Aquivion® ionomer dispersion (D98-06AS), used for the electrode manufacturing, had similar structure and composition of the membrane.

The catalyst-ionomer inks were prepared in order to obtain, after drying, 85 wt. % of IrRuOx catalyst with 15 wt. % of ionomer and 72 wt. % of Pt/C catalyst with 28 wt. % of ionomer, respectively. The cathode ink was in all cases spray coated onto the membrane. In the bare MEA, i.e. an MEA not containing any PtCo recombiner, the IrRuOx anode ink was coated onto the other membrane side. Whereas, in the presence of the recombination catalyst, different approaches were used for the anode manufacturing (see below).

The metal loadings for the bare MEA were 0.3 mg Ir + Ru cm⁻² for the IrRuOx catalyst and 0.1 mg Pt cm⁻² for the Pt/C catalyst.

The activity of the PtCo catalyst for reducing the hydrogen concentration in the anode stream was investigated using two different configurations: “mixed” and “unmixed” configurations referring to a composite anode catalyst layer made of IrRuOx and PtCo or a dual-layer anode with PtCo in between the membrane and the IrRu-oxide layer, respectively (Fig.1).

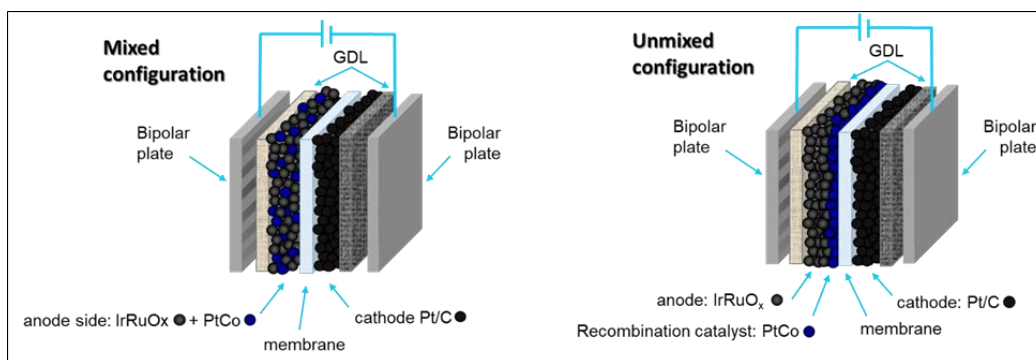


Fig. 1. Structure of the MEAs based on the Pt5.6Co1 recombination catalyst: “mixed” (a) and “unmixed” configuration (b).

In the unmixed configuration, the recombination catalyst ink consisting of 85 wt. PtCo and of 15 wt. ionomer was directly sprayed onto the membrane. Subsequently, the anode layer made of 85 wt. % of IrRuO_x catalyst and 15 wt. % of ionomer was deposited onto the outer surface of the PtCo layer.

The metal loadings for the unmixed configuration were 0.3 mg Ir + Ru cm⁻² for the IrRuO_x catalyst, 0.2 mg Pt cm⁻² for the PtCo catalyst at the anode and 0.1 mg Pt cm⁻² for the Pt/C cathode catalyst.

In the mixed configuration, the recombination catalyst was mixed in a proper amount with the IrRuO_x anode catalyst and the ionomer. The mixed (composite) ink consisting of 85% wt. catalyst and 15% wt. ionomer was spray coated onto the membrane. The metal loadings for the mixed configuration were 0.3 mg Ir + Ru cm⁻² for the IrRuO_x catalyst, 0.2 mg Pt cm⁻² for the PtCo catalyst at the anode and 0.1 mg Pt cm⁻² for the Pt/C cathode catalyst.

A carbon-based gas diffusion layer (GDL ELAT from ETEK) was attached to the cathode side of the CCMs. The assemblies were hot-pressed for 1.5 min at 190 °C and 6 kN to favour the adhesion of the catalytic layers to the membrane. This occurred at a temperature higher than the glass transition temperature of the Aquivion® polymeric membrane (160 °C). The active area (geometrical electrode area) of the MEAs was 8 cm². After the hot-pressing procedure, the membrane-electrode assembly with carbon GDL attached to the cathode, was physically contained between two dense Ti felts. These primarily acted as mechanical support for the MEA. Moreover, the felt at the anode acted as diffusion layer for oxygen evolution. These assemblies were installed in the PEM single cell.

2.4 ELECTROCHEMICAL MEASUREMENTS

Electrochemical measurements were carried out using an in-house developed single cell test station for high differential pressure electrolysis operation equipped with high pressure ITM Power (UK) single cell test fixture and a Varian micro gas-chromatograph for the determination the hydrogen concentration in the oxygen stream at the anode. The single cell electrolysis performance was evaluated at different pressures (atmospheric, 5, 10 and 20 bar) and temperatures (55, 90 and 140 °C). The determination of the hydrogen crossover was carried out under differential pressure i.e. pressurised hydrogen and non-pressurised oxygen at 55 and 90 °C. Thus, the pressure values reported under these conditions are referred to the cathodic compartment only, since the anodic compartment was not pressurised at 55 and 90 °C. At 140 °C, it was necessary to keep constant the anode compartment pressure at 5.5 bar whereas the cathode pressure was varied as in the experiments at lower temperature.

Deionised water (<0.1 μS), further purified by an ion exchange resin cartridge, was supplied by a pump at a flow rate of 1 ml min⁻¹ cm⁻² to the anode compartment. The temperature of the PEM single cell was maintained constant by monitoring the temperature of the recirculating water. This was heated at the specific operating temperature. To avoid water boiling at 140 °C, the anode compartment was pressurised. The water outlet was cooled down before being recirculated through the ion exchange resin.

A power supply (TDK GEN 25400-MD-3P400) was used to perform polarisation experiments in the galvanostatic mode by recording the cell voltage vs. the imposed current density.

An Autolab Metrohm potentiostat / galvanostat equipped with a 20 A current booster and a frequency response analyser (FRA) was used to perform electrochemical impedance spectroscopy (EIS). Electrochemical impedance

analysis was carried out in the potentiostatic mode at 1.5 V and whenever possible also at 1.8 V. The frequency was varied from 100 kHz to 100 MHz in the single sine mode with a sinusoidal excitation signal of 10 mV pk-pk. The activity of the PtCo catalyst was assessed by determining the hydrogen content in the anodic stream (the activity is inversely related to the H₂ concentration). The quantitative analysis of hydrogen concentration was performed at constant current density by an online micro gas-chromatograph (Varian Micro GC). The anodic gas stream was passed through a desiccator before being analysed.

3. RESULTS AND DISCUSSION

The main characteristics of the Pt/C and IrRuO_x electrocatalysts used in the MEAs are reported in Table 1. The focus of this work is essentially regarding the PtCo catalytic recombiner.

3.1 MICROSTRUCTURE AND MORPHOLOGY OF THE UNSUPPORTED PtCo RECOMBINATION CATALYST

The atomic ratio for the PtCo alloy was investigated by EDX measurements. With respect to the PtCo catalyst reported in a previous study (D4.3), a different preparation procedure was used. This provided enhanced catalyst properties in terms of small crystalline size and better alloying between Pt and Co. In effect, the unalloyed Co species were removed through a strong pre-leaching treatment in acid. A bulk composition of 85:15 at. % of Pt:Co was obtained after an optimisation of the post-synthesis treatments. A lower reduction temperature and a pre-leaching treatment in an acidic solution five times more concentrated than that previously used (D4.3) were adopted. The aim was to achieve a platinum enrichment on the surface to improve the stability of the catalyst under anodic operating conditions.

Fig. 2 shows the occurrence of a face-centred cubic crystallographic structure of Platinum (JCPDS card no. 4-802) for the PtCo catalyst. The peaks show a significant shift towards higher Bragg angles with respect to the diffraction pattern of platinum. The lattice constant for the PtCo alloy is determined from the inset in Fig. 2 ($a_{220}=0.3865$ nm). The corresponding estimated atomic content of Co in the alloy from the Vegard's law is about 15 ± 2 % that is close to the nominal amount. No peaks related to other crystalline phases are detected for the catalyst. The average crystallite size as estimated by the Debye-Scherrer equation is 4 nm. A significant reduction of the crystallite size with respect to our previous recombination catalyst (around 10 nm) is observed.

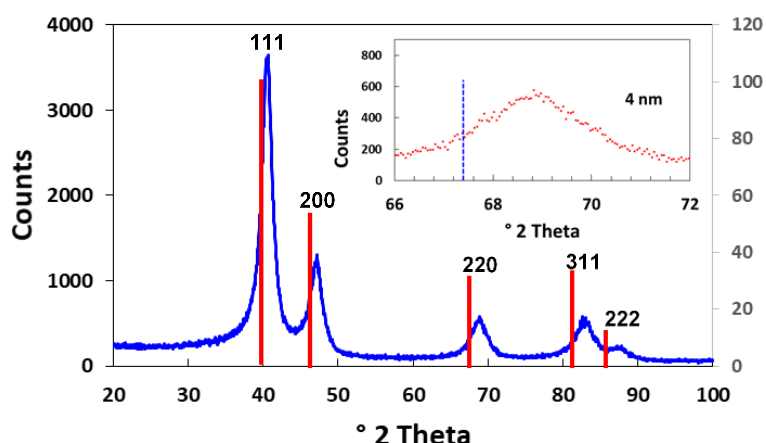


Fig. 2 X-ray diffraction patterns of Pt_{5.6}Co₁ catalyst and face centred cubic Pt as reference, JCPDS card no. 4-802. The inset shows the 220 peak broadening used for determining the mean crystallite size.

The morphology of the catalyst was investigated by SEM and TEM analyses. The SEM image in Fig. 3 shows a porous sponge-like morphology. The inset in Fig. 3 relates to a TEM micrograph of the PtCo catalyst, which is composed of nanoparticles of spherical shape. The image depicts a relevant agglomeration that is a typical feature of unsupported catalysts. This does not allow proper determination of the particle size distribution.

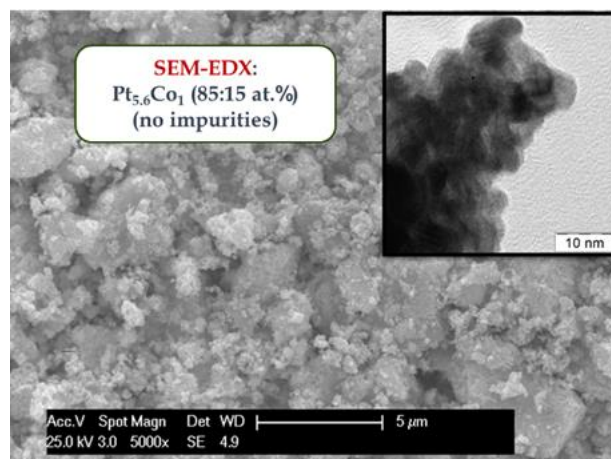


Fig. 3. SEM and TEM (inset) micrographs of the PtCo catalyst.

3.2 SURFACE CHARACTERISATION OF THE PtCo CATALYST

The surface atomic composition of the PtCo recombination catalyst was investigated by XPS analysis. XP survey spectra of the pristine and sputtered Pt_{5.6}Co₁ catalyst (Fig. 4) revealed a prevailing occurrence of platinum on the surface, with a surface atomic composition of Pt:Co = 90:10.

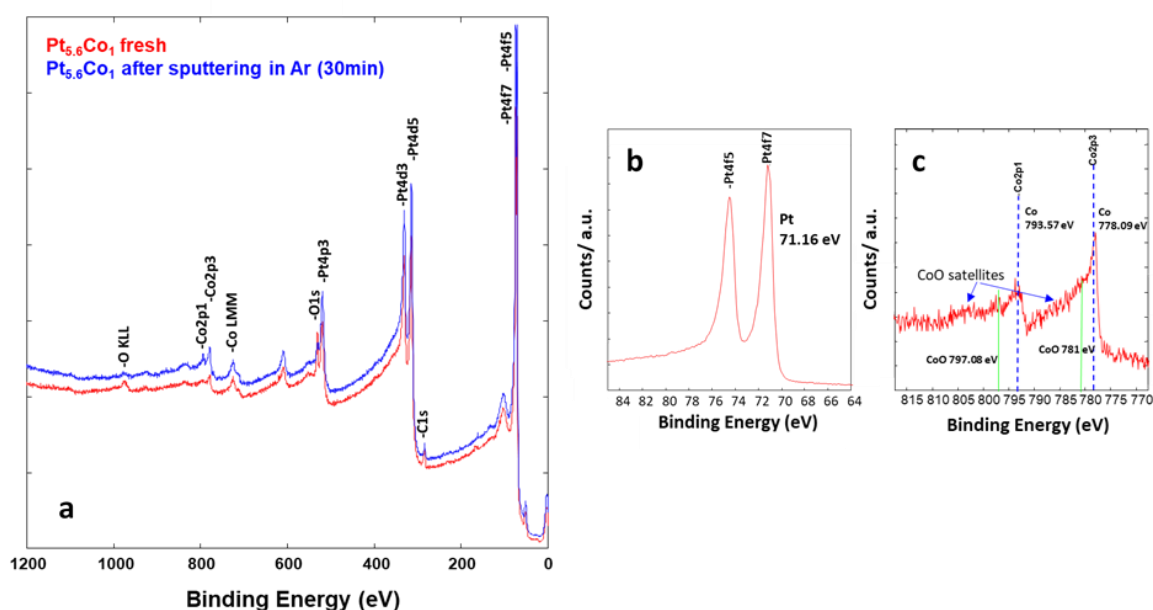


Fig. 4. Survey XP spectrum of the pristine and sputtered Pt_{5.6}Co₁ catalyst (a), high resolution XPS spectra of Pt 4f (b) and Co 2p (c).

After a sputtering treatment with argon ions at 5 kV for 30 min., the cobalt concentration on the surface increased reaching the EDX-determined bulk composition (Pt:Co = 85:15 %at). The O1s and C1s signals are related to adventitious carbon-containing species as confirmed by a significant decrease of such signals after sputtering. High-resolution XPS spectra of the fresh catalyst show the prevailing occurrence of metallic Pt and Co on the surface. The contribution of cobalt oxide (CoO) to the overall Co2p spectrum was relatively low compared to metallic cobalt. The main peaks of CoO are indicated by full lines in Fig. 4c. Satellite peaks usually associated with the paramagnetic CoO are just slightly envisaged and are indicated by arrows (Fig. 4c). Thus, there is a slight presence of CoO but in a

modest amount compared to metallic Co. The effect of Co in this catalyst is to favour a charge transfer to Pt. The surface properties of the IrRuOx catalyst is, essentially, characterised by an enrichment of Ir on the surface.

3.3 SINGLE CELL ELECTROCHEMICAL ASSESSMENT OF THE Pt-Co ALLOY CATALYST FOR THE REDUCTION OF THE HYDROGEN CONCENTRATION IN THE OXYGEN STREAM

As reported in Fig.1, two different MEA structures (mixed and unmixed), based on the use of a PtCo recombination catalyst (RC) at the anode, were investigated. Fig. 5 shows a comparison of the H₂ content in the oxygen stream as function of the current density at a constant temperature of 55°C and at two different differential pressures (pressurised H₂, non-pressurised O₂) i.e. 10 and 20 bar. To evaluate the progress made in this work, the two configurations based on the present recombination catalyst and a thin 50 µm Aquivion (E98-05S) membrane were compared to an unmixed (double-layer anode) MEA based on a 90 µm Aquivion (E98-09S) membrane and containing our first version of a PtCo recombination catalyst. The aim was to understand the enhanced activity of the present catalyst under more harsh conditions determined by the presence of a thinner membrane causing larger hydrogen crossover. At 55 °C, in all configurations, the H₂ concentration was relatively high at very low current densities (Fig. 5). However, it progressively decreased once the production of oxygen increased with the current density and thus the permeated hydrogen at the anode was diluted. The lowest H₂ concentration in the oxygen stream was recorded, in the overall range of current density, for the MEA based on the present PtCo recombination catalyst (RC) mixed with the IrRuOx oxygen evolution catalyst. The H₂ concentration was kept below 2.5 % also at high differential pressure (20 bar) and at a low current density of 0.2 A cm⁻² corresponding to 5% of partial load for an electrolysis system operating at a nominal current of 4 A cm⁻². It is interesting to observe that even using the unmixed approach, the new PtCo catalyst shows better capability to reduce the hydrogen concentration than the previously developed PtCo, under the same configuration (Fig. 5). This is evident under critical low load conditions (low current density) despite the smaller membrane thickness (50 vs 90 µm) of the present MEA and the consequently larger H₂ crossover compared to the previously developed MEAs. This was attributed to the smaller crystallite size and better degree of alloying of the present catalytic recombiner compared to our previous PtCo catalyst (D4.3). Moreover, it is worth mentioning that the Pt4f7/2 binding energy for the present catalyst was 71.16 eV compared to 71.30 eV of the previously developed catalyst (Table 1). This indicates better metallic properties and larger charge transfer from Co to Pt for the present catalytic system. These characteristics make Pt sites on the surface less prone to surface oxidation under electrolysis conditions. This property is fundamental for a more efficient adsorption of the permeated hydrogen molecules on the PtCo surface. The adsorbed molecules are thus oxidised to protons by effect of the high electrochemical potential or to water by the oxygen evolved at the neighbouring IrRuOx catalyst according to a chemical recombination process. The electrochemical oxidation of H₂ appears more effective in the unmixed (double layer anode) configuration; whereas, the mixed (composite catalyst layer) configuration should promote the direct recombination with the oxygen molecules evolved at the neighbouring catalytic sites.

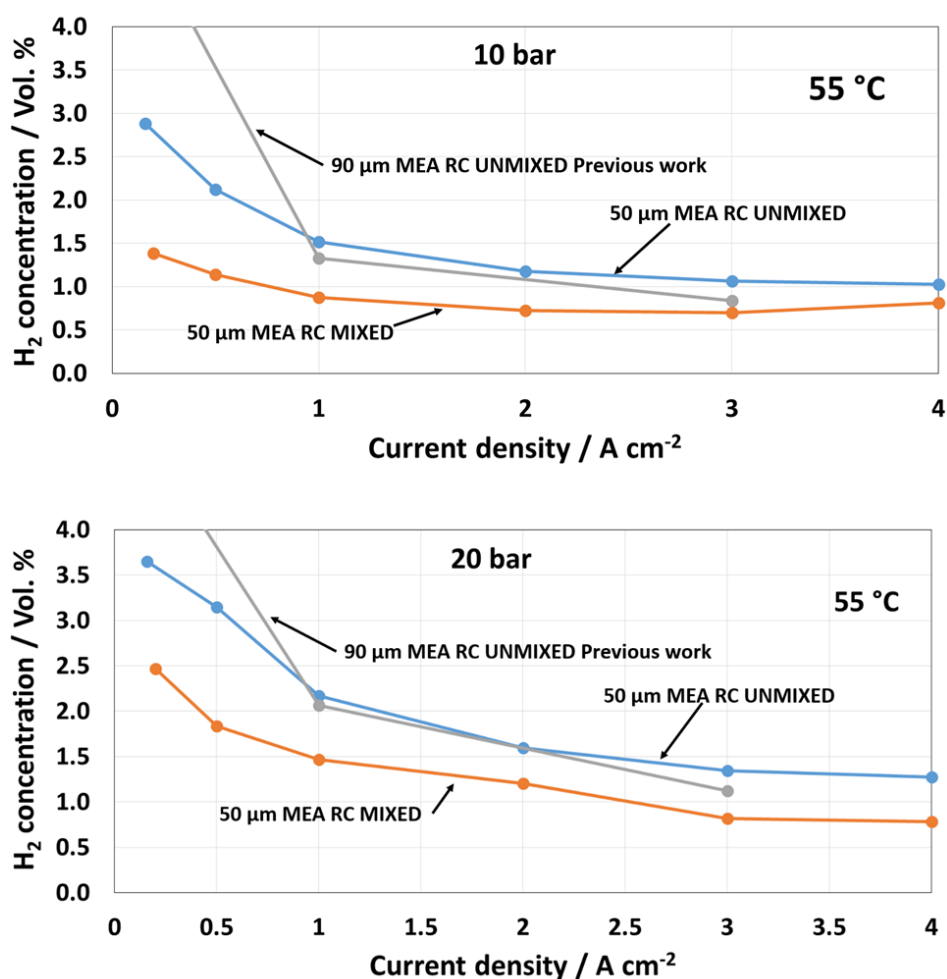


Fig. 5. H₂ concentration in the anodic oxygen stream at different current densities for various MEA configurations, at 55 °C, 10 and 20 bar differential pressure. RC refers to the PtCo recombination catalyst.

Fig. 6 shows a comparison of the polarisation curves for the different MEAs at 55 °C, 10 bar differential pressure. The electrochemical tests showed lower cell voltage at the same current density for the MEAs based on the unmixed configuration, both using the old and new version of recombination catalysts. It is clearly observed that the mixed configuration, containing a composite anode catalyst layer, is characterized by a lower voltage efficiency compared to the two separate anodic layers. It is speculated that when the Pt sites are mixed to Ir and Ru catalytic sites, these can affect negatively the oxygen evolution reaction, Pt being less active than Ir- and Ru-oxide. It is also noted that despite the different membrane thickness, the MEA based on the thin E98-05 membrane performs only slightly better at 10 bar and essentially similar at 20 bar compared to the MEA based on the thick E98-09 membrane. This may depend on the different membrane forming procedures causing slightly different protonic conductivity as well as the MEA fabrication producing better mechanical compression in the case of the E98-09 membrane. The mixed configuration appears superior to the unmixed approach in terms of reducing the concentration of hydrogen in the oxygen stream possibly due the different reaction mechanisms discussed above (chemical recombination vs. electrochemical oxidation). Moreover, the new PtCo catalyst allows reducing the H₂ content at the anode at the same extent of the previous PtCo system in the presence of a much thinner membrane (50 vs 90 microns) (Fig. 5).

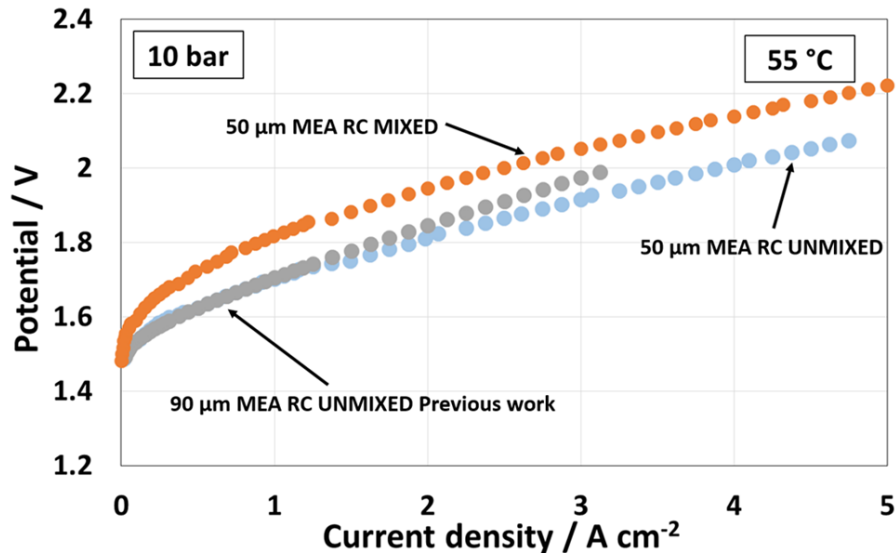


Fig. 6. Polarization curves for various MEA configurations, at 55 °C, 10 bar differential pressure. RC refers to the PtCo recombination catalyst.

Fig. 7 shows a comparison at 90°C between the mixed and unmixed configurations in terms of electrochemical performance (Fig. 7a) and activity for reducing the hydrogen concentration (Fig. 7b) at the anode. Also, at 90°C, the PtCo catalyst in the mixed configuration shows a lower electrochemical performance than the unmixed one. The H₂ concentration in O₂ was still lower for the recombination catalyst mixed configuration (as observed at 55 °C). The RC unmixed configuration showed interesting electrochemical performance at 20 bar and 90°C (~1.87 V at 4 A cm⁻²) but relatively high H₂ concentration in O₂ at low current density (Fig. 7). The H₂ concentration in O₂ was relatively high at 20 bar and 90°C, about 3.3 % at 1 A cm⁻², for the thin 50 μm Aquivion® membrane equipped with the catalytic recombiner in the dual layer anode (Fig. 7). Thus, for the latter configuration operating with a nominal operating current density of 4 A cm⁻², the minimum applicable load is about 25%. Whereas, if the mixed configuration is preferred (Fig. 7), assuming, also in this case, a nominal operating current density of 4 A cm⁻², as a proper compromise between efficiency and production rate, the minimum partial load operation can be as low as 5% (0.2 A cm⁻²). This can provide a significant improvement of the dynamic behaviour of thin-membrane based electrolyzers with just a slight loss of voltage efficiency at the nominal current density (~4% i.e. from 79% unmixed to 75% mixed configuration).

The different capability of reducing the H₂ concentration in O₂ for these two configurations appears quite significant at 90 °C suggesting that an increase of temperature may also favour the chemical recombination process (composite catalyst approach) compared to the electrochemical oxidation of hydrogen to protons (unmixed approach).

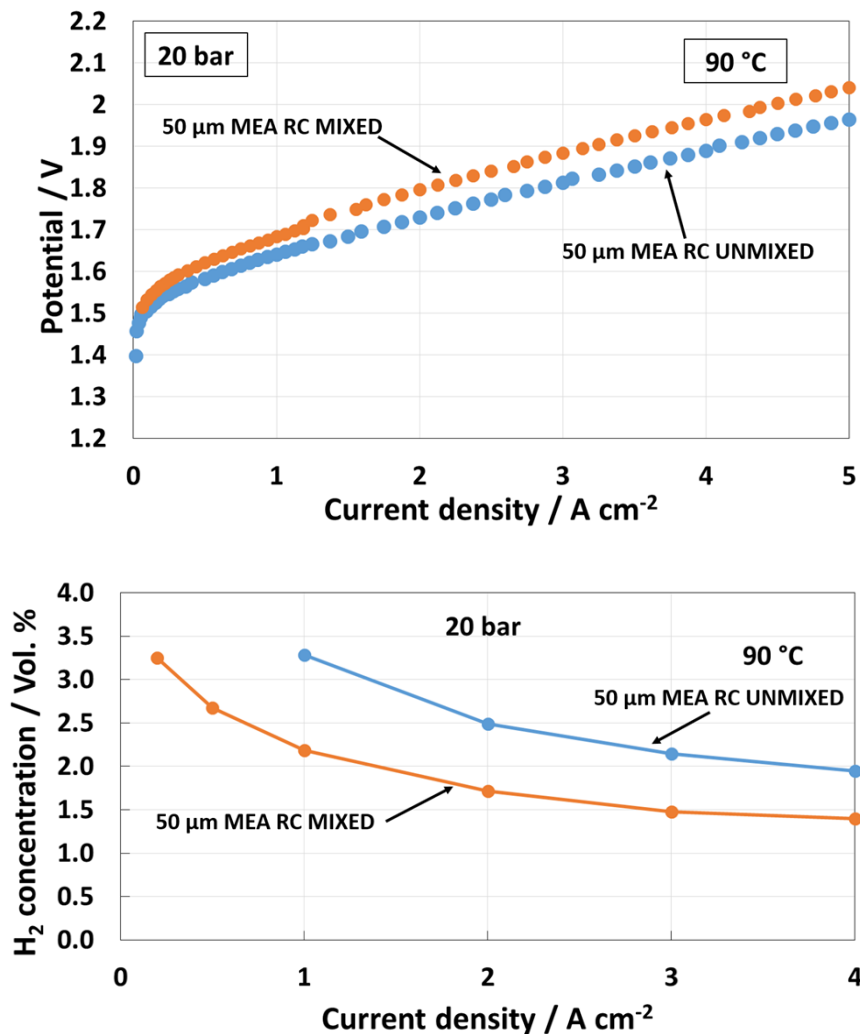


Fig. 7. Polarization curves and H₂ concentration in O₂ for RC MIXED and UNMIXED based MEAs.

Fig. 8 shows that, at 55 °C, the MEA containing the PtCo catalyst at the anode, even in the mixed configuration, is performing better in terms of voltage efficiency compared to a bare MEA based on the same membrane. Thus, two effects are played by the recombination catalyst i.e. reduction of H₂ concentration in O₂ and slight increase of electrochemical performance. The increase of performance may be in part due to a depolarisation effect (hydrogen oxidation instead of oxygen evolution over the PtCo catalyst) and in part to a contribution to the oxygen evolution. However, the addition of the catalytic recombiner also means a larger loading of precious group metals (0.6 vs. 0.4 mg PGM cm⁻²_{MEA}). The larger PGM loading in the MEA containing the PtCo catalyst may allow a better current collection for such a thin catalyst layer compared to the bare MEA. However, impedance studies in Fig. 8 do not show relevant change in series resistance. Whereas a variation of the polarisation resistance is clearly observed. A lower polarisation resistance for the PtCo based MEA is effectively observed at 1.5 V but it is even more evident at higher cell voltages (1.8 V) corresponding to higher current density. Under these conditions, the hydrogen permeation rate is higher and the PtCo catalyst contributes to depolarizing the anode by oxidation of the permeated H₂.

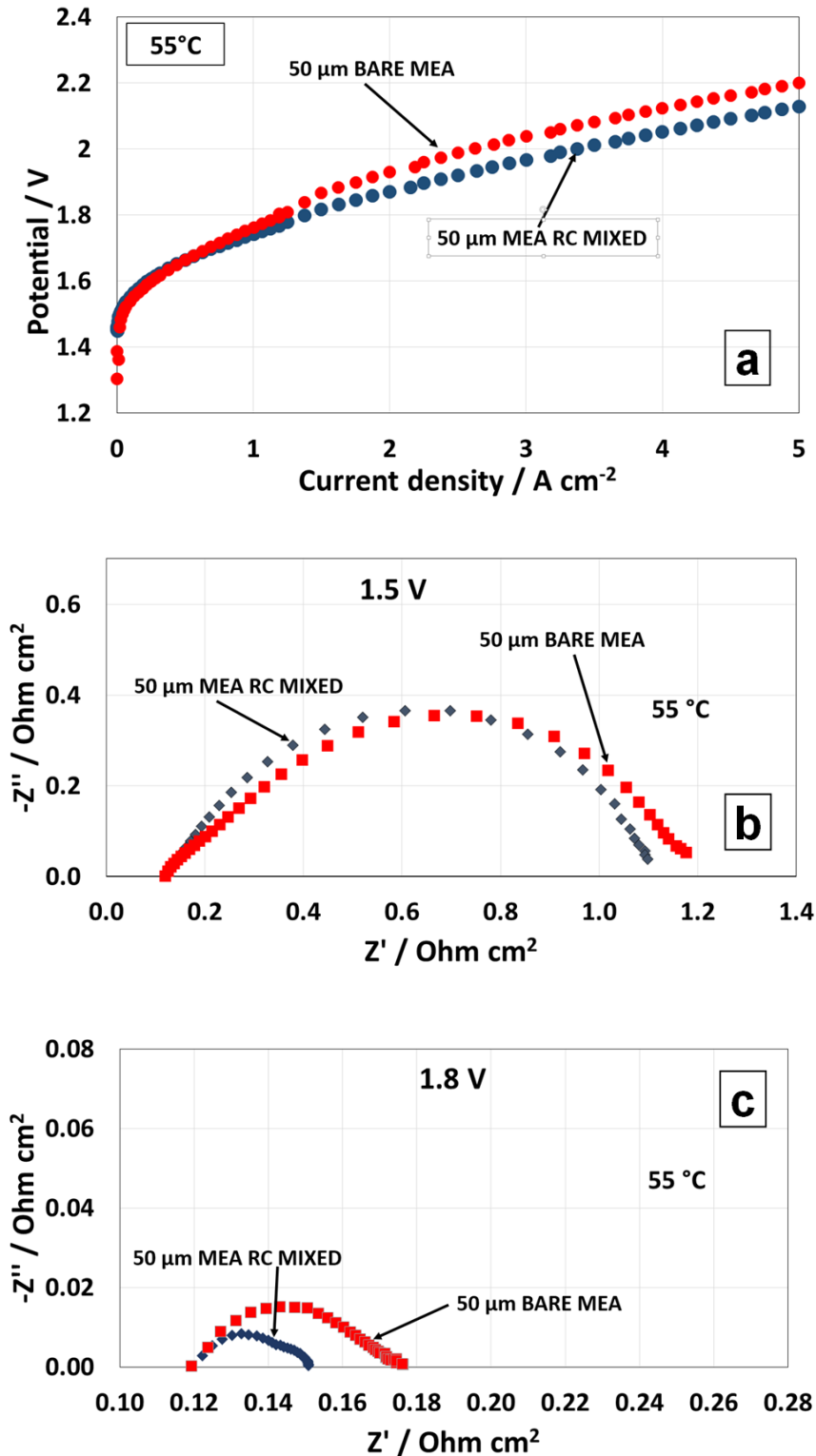


Fig. 8 Polarization curves (a) and impedance spectroscopy at 1.5 V (b) and 1.8 V (c) comparison for bare and RC MIXED configuration based MEAs.

For the same configuration, e.g. mixed catalyst layer, the H₂ concentration was higher at 90° C compared to 55° C (Fig. 9). This behaviour is essentially due to the larger membrane swelling at 90°C causing an increase of gas crossover. An increase of temperature improves the voltage efficiency but it also increases the permeation rate and thus the content of H₂ in the oxygen stream (Fig. 9).

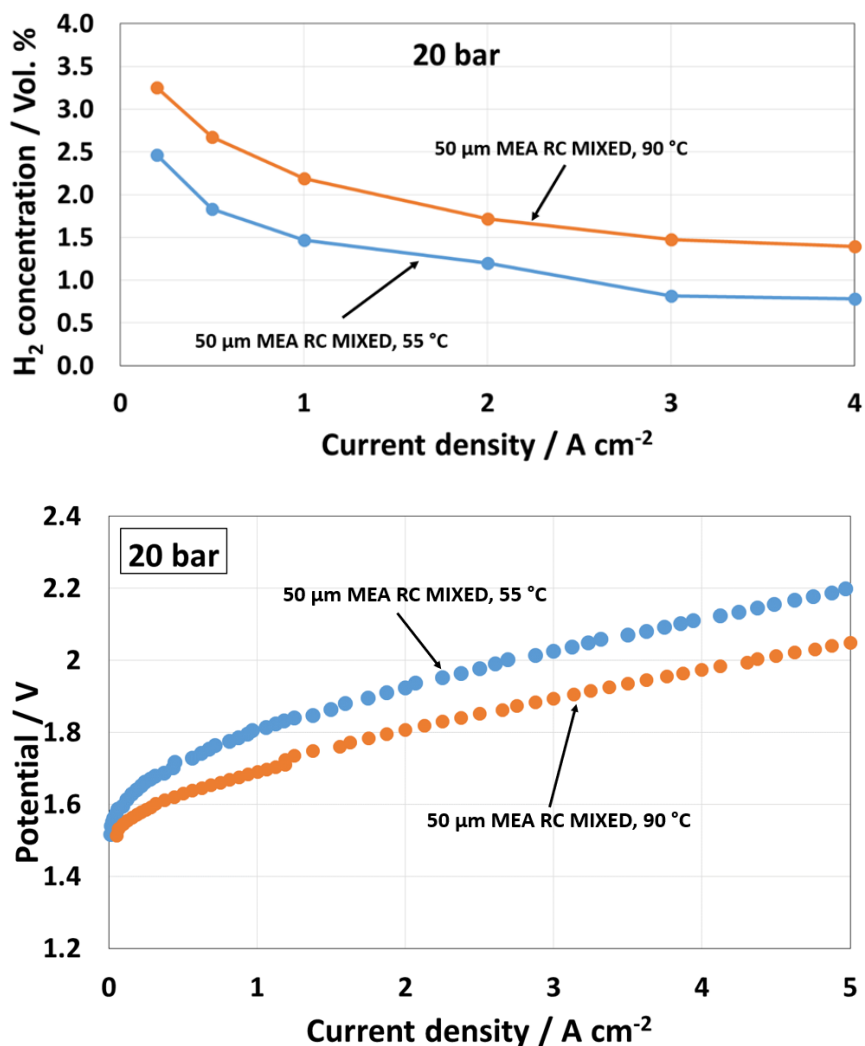


Fig. 9 Polarization curves and H₂ concentration in O₂ comparison at different temperature for the RC MIXED configuration-based MEA.

The Aquivion® membrane is characterised by a high glass transition temperature allowing, in principle, operation at intermediate temperatures. Operation at 140 °C is an interesting trade-off because of the more favourable thermodynamic conditions, enhanced reactions kinetics and lower cooling requirements while avoiding negative effects on the membrane mechanical stability.

However, above 100 °C, the rapid water evaporation from the membrane causes a significant decrease of its proton conduction. Thus, operation at temperatures above 100 °C is only possible if the cell is properly pressurised. In our PEM configuration, with water supplied only to the anode, this compartment needs to be pressurised for operation at temperatures larger than 100 °C. The cathodic layer is kept humidified by the water diffusion through the membrane. This occurs by the effect of the water concentration gradient between anode and cathode. Beside the anode, pressurisation of the cathode also helps in keeping liquid water inside the cell at temperatures above 100 °C. Thus, during PEM electrolysis operation at 140 °C, it was necessary to keep constant the anode compartment pressure at 5.5 bar abs. whereas the cathode pressure was varied as in the experiments carried out at lower temperature.

At 140 °C, the electrochemical performance at high current densities, with the cathode kept at ambient pressure, was worse than at higher cathode pressures probably due to the relevant presence of water vapour in the gas phase (Fig. 10). Water permeation from anode to cathode at 140°C produced indeed a quick water vaporization at the cathode kept at ambient pressure causing mass transfer constraints for hydrogen evolution. This is particularly evident at high current density and it influences negatively the cell efficiency (Fig. 10). The trend between 10 and 20 bar was in line with that observed at lower temperatures i.e. the cell voltage was increasing slightly as the

pressure was increased according to the Nernst law. In this case, the pressurization of the cathode allowed to keep the permeated water in a liquid form favouring hydrogen gas separation from the liquid phase. Impedance spectra were carried out at 1.5 V only, because at 1.8 V, the electrical current at 140 °C exceeded the limit of the ac-impedance analysis booster. However, also impedance spectroscopy confirmed this peculiar trend at intermediate currents. Polarisation resistance decreased by decreasing the cathode pressure from 20 to 10 bar and increased again at ambient cathode pressure.

At very low current density and at ambient cathode pressure, the presence of water vapour did not hinder much the hydrogen evolution because of the small production rate. It is noted that at 140 °C, under pressurised conditions, e.g. 20 bar cathode, 5.5 bar anode, at 5 A cm⁻², the cell voltage was as low as 1.8 V. This represents a significant gain in cell performance showing the importance of operation at intermediate temperatures.

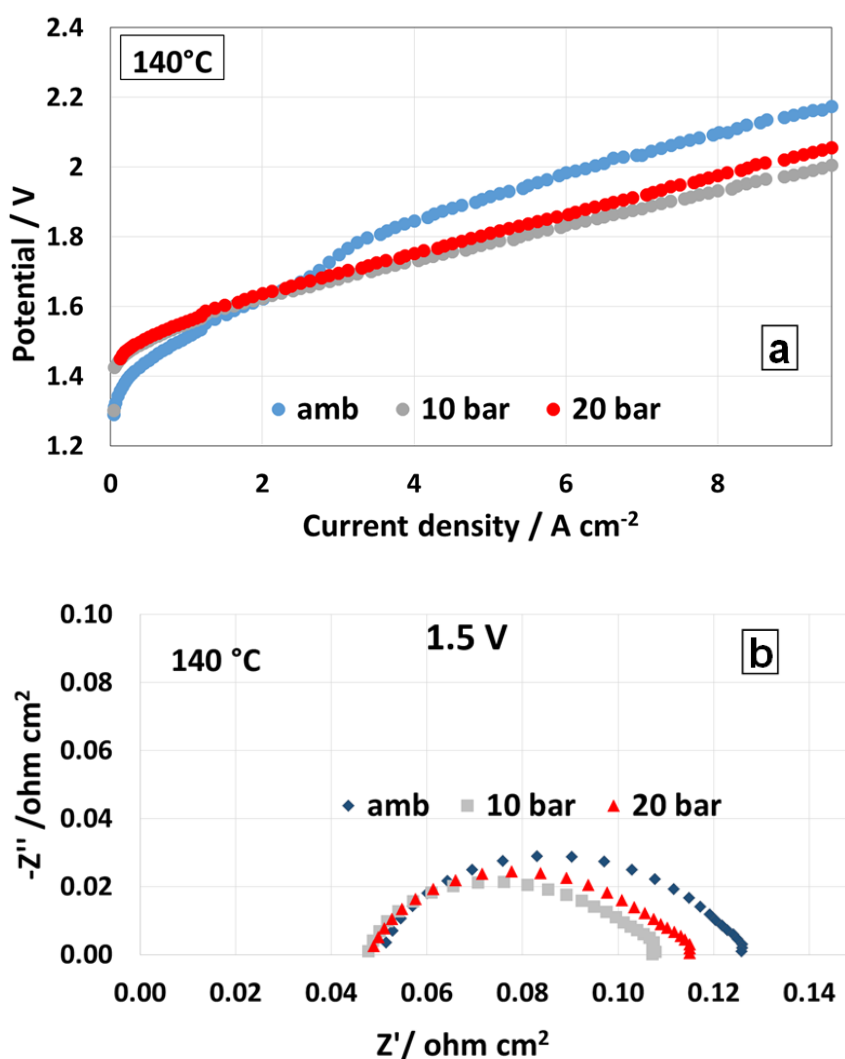


Fig. 10 Polarization curves (a) and impedance spectroscopy (b) comparison at 140°C and different cathodic pressures for RC MIXED MEA. The anode pressure was kept constant at 5.5 bar.

It is now useful to analyse the effect of the operating cell temperature on the hydrogen concentration in the oxygen stream. Fig. 11 shows the tests carried out from 55 °C to 140 °C under the conditions discussed above (ambient pressure is used at the anode until 90 °C and it is increased to 5.5 bar abs at 140 °C). An increase of temperature caused an increase of the H₂ concentration in O₂ when passing from 55 °C to 90 °C. However, a different behaviour was observed at 140 °C. The H₂ crossover under differential pressure operation (with the cathode kept at higher pressure than the anode) was relatively constant from low to high current density. It is important to consider that the anode pressurisation promotes the recombination process over the recombination catalyst surface.

However, this trend was not observed when the cathode was kept at ambient pressure. An unusual increase of hydrogen concentration with the current density was observed. Of course, this appears associated to the increase of the hydrogen permeation rate with the increase of current density but the usual prevailing counteracting effect of the hydrogen dilution caused by the increased oxygen evolution was less relevant in this situation.

In principle, this trend was in part caused by the very efficient behaviour of the recombination catalyst in the presence of pressurised oxygen (5.5 bar) at 140 °C especially at low current density and ambient cathode pressure when the hydrogen permeation rate was relatively low. Under these conditions, the evolved H₂ gas needs to compete with water vapour (ambient cathode pressure) to permeate to the anode. The pressurised oxygen at the anode produces a differential pressure with an opposite direction acting as physical barrier. All these phenomena were probably impeding relevant amounts of hydrogen to permeate to the anode at low current density and the few permeated molecules were also efficiently oxidised by the recombination catalyst. Upon increasing the current density to certain values, the hydrogen permeation increased significantly because of the supersaturation of the cathode catalytic layer causing the observed increase of H₂ concentration in O₂. Thus, this trend is essentially determined by a trade-off between the increased hydrogen permeation rate, caused by the increase in current density, and the counteracting activity of the recombination catalyst at high temperature that is especially high in the presence of low H₂ permeation values.

When the cathode was also pressurised at 140 °C, an increased H₂ permeation occurred already at low current densities by the pressure effect. Under these conditions, the larger H₂ permeation was less counteracted by the activity of the recombination catalyst even if this was still promoted by the presence of a small oxygen pressure at the anode. Upon pressurisation of the cathode at 140 °C, the relevant effects were an increased hydrogen permeation rate, the dilution of the permeated hydrogen by the evolved oxygen, the still relevant activity of the recombination catalyst and the transport of liquid water to the cathode (electroosmotic drag) associated to the increase of current density. These phenomena possibly compensated each other and the H₂ concentration in O₂ remained almost constant with the current density. Moreover, the higher catalyst activity observed at 140 °C in comparison to lower temperatures has a positive effect on reducing the H₂ concentration by balancing the negative effects of membrane swelling.

Regarding the effect of the cathode pressure, a usual trend was observed at 55 °C with the concentration of H₂ in the anodic stream decreasing as a function of the increase of current density and decrease of pressure (Fig. 11a). At 90 °C (Fig. 11b), the enhanced activity of the recombination catalyst caused a change of this trend especially at low current densities and low cathodic pressures when the H₂ permeation rate was low. At 90 °C and ambient pressure, the H₂ concentration in O₂ was very low at low current density and increased with the increase of H₂ production rate. This phenomenon was relatively similar to that occurring at 140 °C and already commented. At 140 °C this was more evident where the activity of the recombination catalyst was further enhanced by the temperature and mild anode pressurization, as required to avoid water boiling (Fig. 11c).

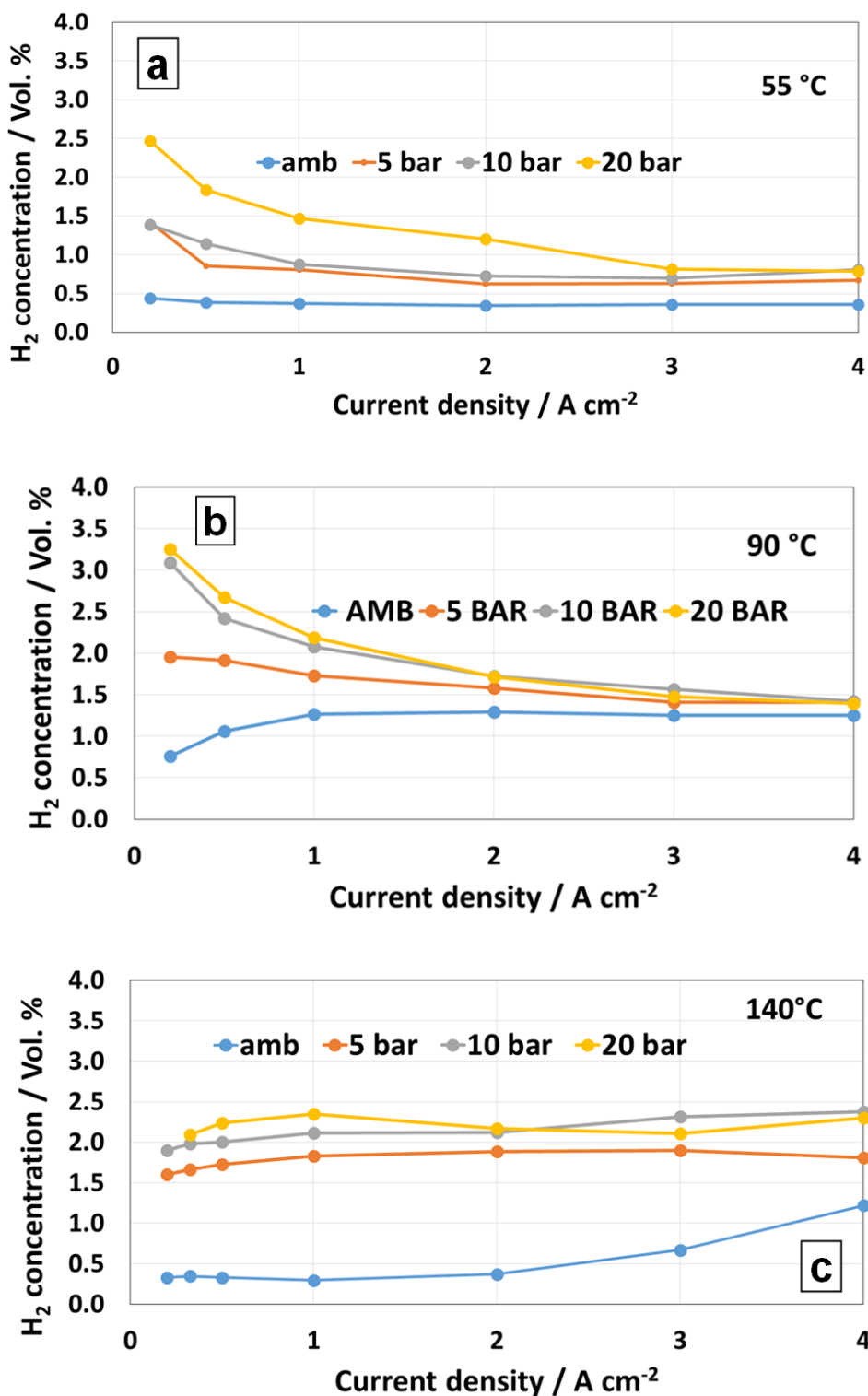


Fig. 11 Comparison of the H₂ concentration in O₂ at different temperatures and pressures for MIXED RC based MEA. Ambient anode pressure was used at 55 °C and 90 °C whereas a pressure of 5.5 bar was used at 140 °C.

The effect of pressure on the electrochemical performances of the MEA containing the recombination catalyst in a mixed configuration at 55 °C is shown in Fig. 12. Under these specific operative conditions, a pressure increase from 0 to 10-20 bar caused an increase of cell voltage as expected from the Nernst equation. This is more evident in the impedance spectra where an increase of polarization resistance with pressure is observed at two different potentials 1.5 V and 1.8 V.

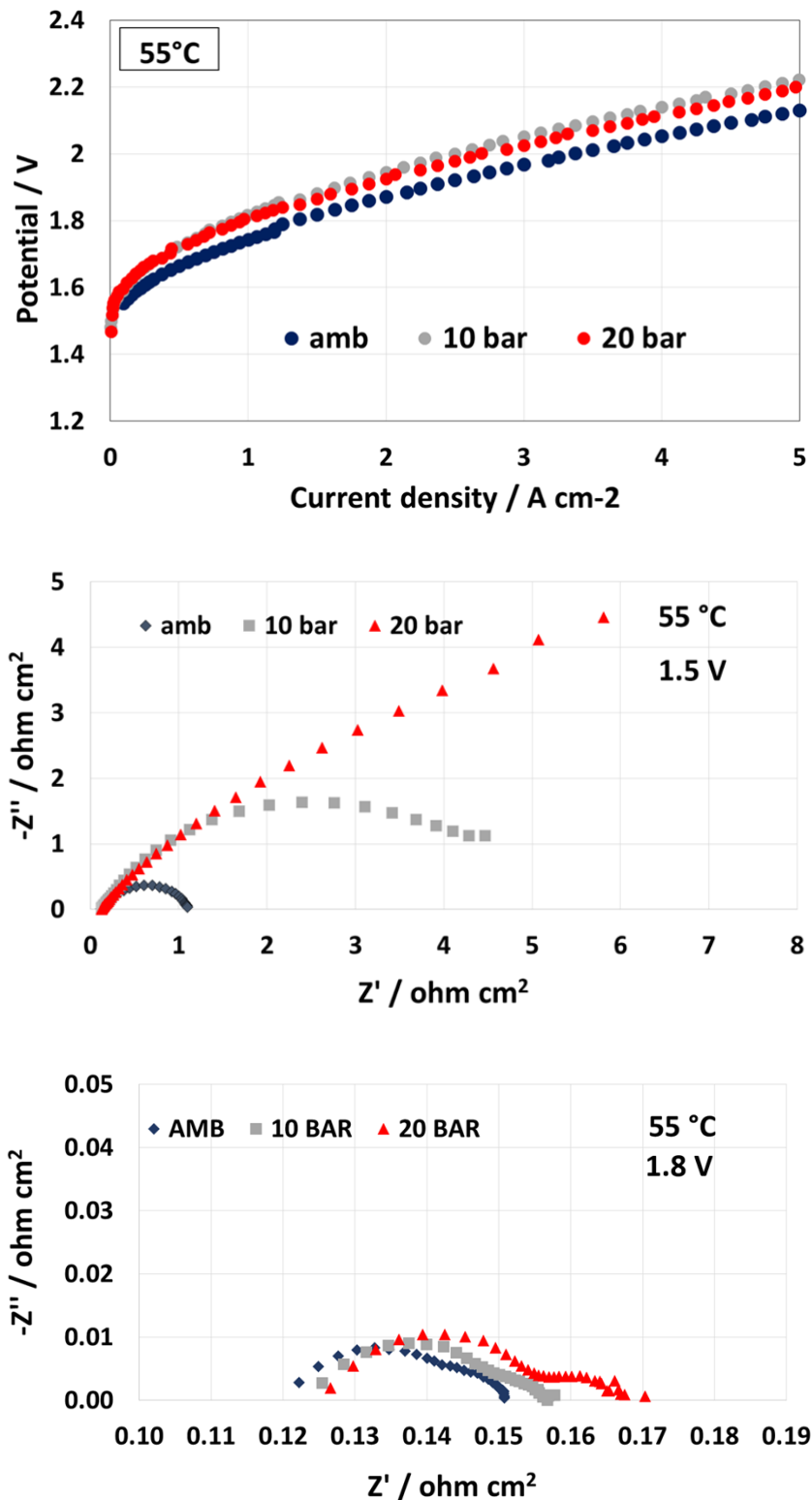


Fig. 12 Comparison of polarization curves and impedance spectra at 55°C and different pressure for RC-based mixed MEA.

The effect of the cathodic pressure was smaller at 90 °C with similar electrochemical performances in the analysed pressure range (Fig. 13). The impedance spectra still showed larger polarization resistance with the increase of pressure at 90 °C according to the Nernst law. This was more evident at 1.5 V where the shift in the Nernst potential had a larger impact on the polarization resistance. Such features were amplified by the impedance spectroscopy analysis whereas minimal effects were observed in the polarization curves. In general, the increase of pressure has a modest effect on the electrolyser voltage efficiency whereas it allows reducing significantly the energy

consumption of the downstream mechanical gas compression especially in refuelling stations applications. It appears that a further increase of the operating differential pressure in PEM electrolysis, in the presence of thin membranes, can be sustained by a proper development of the integrated recombination catalyst technology.

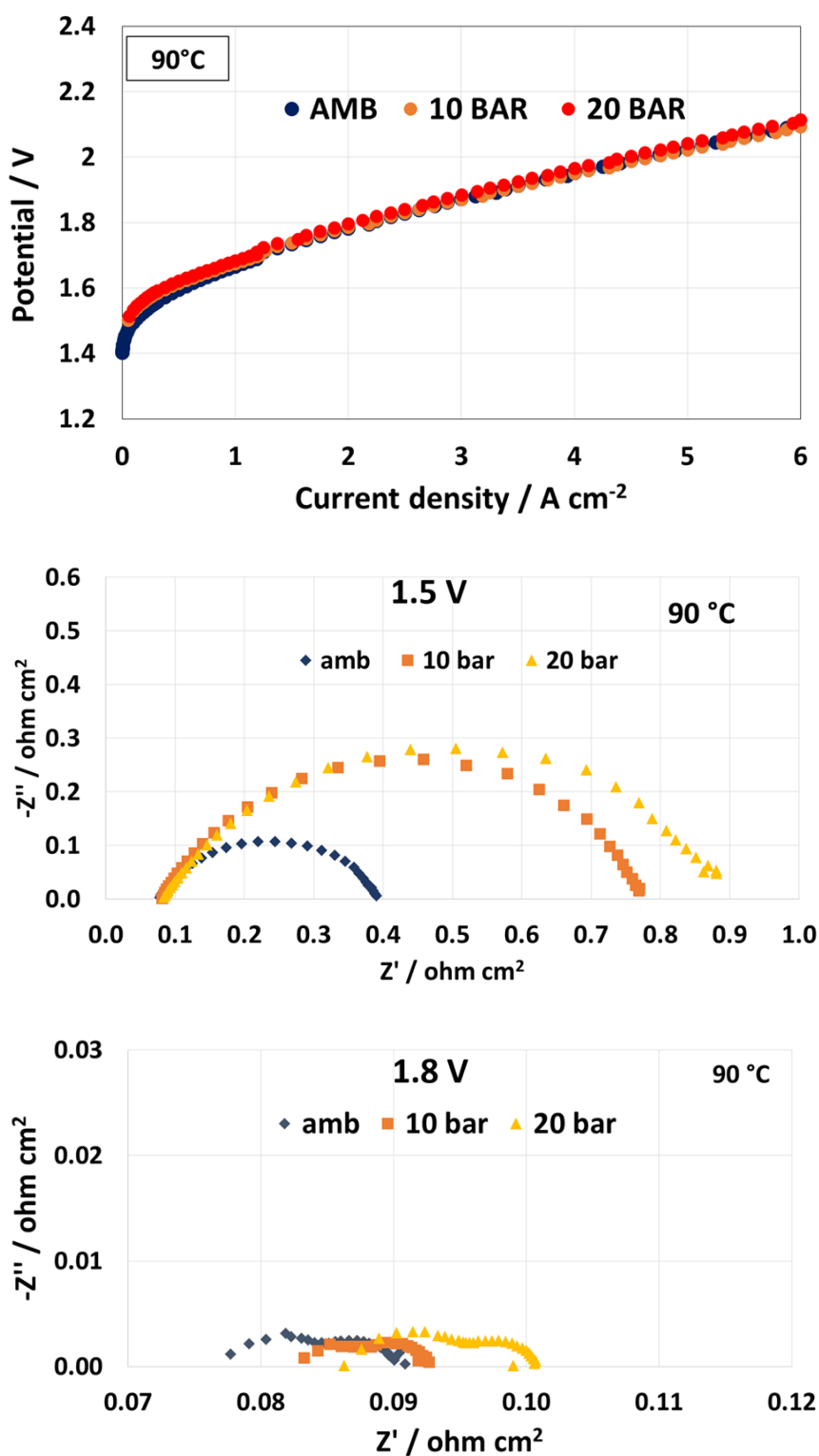


Fig. 13 Comparison of polarization curves and impedance spectra at 90 °C and different pressure for RC-based mixed MEA.

4. CONCLUSIONS

A PtCo alloy recombination catalyst was integrated in a membrane-electrode assembly and investigated for reducing the H₂ concentration in the oxygen stream during PEM electrolysis operation in the presence of a thin 50 µm PFSA Aquivion® membrane. The PtCo catalyst properties were optimised to provide enhanced activity through tailoring the catalytic recombiner surface chemistry, electronic effects and mean crystallite size.

Two different MEA configurations were studied. A dual-layer (unmixed) anode configuration where the PtCo alloy catalyst was integrated in the membrane-electrode assembly between the membrane and the IrRuOx anode catalyst and a mixed layer (composite anode layer) configuration made of a mixture of PtCo and IrRuOx. Both configurations showed good performance for the oxidation of the permeated hydrogen allowing to achieve enhanced safety characteristics under differential pressure. The mixed configuration showed better activity for reducing the hydrogen concentration at the anode but slightly lower electrochemical performance. Two mechanisms were hypothesized: one mainly consisting of an electrochemical oxidation of the permeated H₂ to protons (unmixed configuration) and the other consisting of a direct chemical recombination mechanism (mixed configuration) of the permeated hydrogen and evolved oxygen into water. The performance of the MEAs containing the recombination catalyst was better than a bare MEA while producing a decrease of the H₂ content at the anode. This allowed extending the load range under differential pressure. The effects of the cathodic pressure and cell temperature on the electrochemical performance and H₂ content at the anode were investigated. At 55 °C and 20 bar differential pressure, in the presence of the PtCo catalytic recombiner and a thin 50 µm PFSA membrane, the hydrogen concentration in the anodic oxygen stream was well below the flammability limit at a current density as low as 0.2 A cm⁻². This corresponds to about 5 % partial load operation for a nominal operating current density of 4 A cm⁻² corresponding to about 70 % voltage efficiency at 55 °C. An enhancement of the dynamic characteristics for PEM electrolysis is expected compared to conventional systems (minimum load range of 20 %).

The mixed configuration was also investigated at an intermediate operating temperature of 140 °C at different cathodic pressures using a slightly pressurised anode. An excellent performance of 4 A cm⁻² at 1.75 V at 140 °C, 20 bar cathode pressure and 5.5 bar anode pressure was recorded. This performance was achieved in the presence of a H₂ concentration in the oxygen stream of about 2 % that was almost constant through the overall current density range. Such results indicate good perspectives for intermediate temperature PEM electrolysis operation using thin membranes in order to increase electrochemical efficiency, reduce energy consumption for cooling and make better use of the higher quality heat released under electrolysis operation at high current density.

ACKNOWLEDGEMENTS

The authors acknowledge the financial support from the NEPTUNE project. This project has received funding from Fuel Cells and Hydrogen 2 Joint Undertaking under grant agreement N 779540. This Joint Undertaking receives support from the European Union's Horizon 2020 research and innovation programme and Hydrogen Europe and Hydrogen Europe Research